Towards an Appropriate Beamforming Scheme for Initial Cell Discovery in mmW 5G Cellular Networks

Waqas bin Abbas, Michele Zorzi
Department of Information Engineering, University of Padova — via Gradenigo 6/B, 35131 Padova, Italy
E-mail: {waqas,zorzi}@dei.unipd.it

arXiv:1605.00508v1 [cs.IT] 2 May 2016

***Abstract*—Beamforming is an essential requirement to combat high pathloss and to improve signal-to-noise ratio during initial cell discovery in future millimeter wave cellular networks. The choice of an appropriate beamforming is directly coupled with its energy consumption. The energy consumption is even of more concern at a battery limited mobile station (MS). In this work, we provide an energy consumption based comparison of different beamforming schemes while considering both a low power and a high power analog-to-digital converter (ADC) for a millimeter wave based receiver at the MS. We analyze both context information (CI) (GPS positioning based) and non context information based schemes, and show that analog beamforming with CI (where mobile station's positioning information is already available) can result in a lower energy consumption, while in all other scenarios digital beamforming has a lower energy consumption than analog and hybrid beamforming. We also show that under certain scenarios recently proposed phase shifters network architecture can result in a lower energy consumption than other beamforming schemes. Moreover, we show that the energy consumption trend among different beamforming schemes is valid irrespective of the number of ADC bits. Finally, we propose a new signaling structure which utilizes a relatively higher frequency sub-carrier for primary synchronization signals compared to other signaling, which allows a further reduction in initial cell search delay and energy consumption of the MS.**

I. Introduction

At millimeter wave (mmW) huge bandwidths are available to fulfill the data rate requirement of the next generation (5G) cellular networks [1]. However, unlike in microwave bands, mmW communication suffers from high path-loss [2]. To address this issue, spatial beamforming is considered as an inevitable choice for mmW communication [3]. Unlike in LTE, beamforming (BF) in mmW communication is not only an essential requirement for data plane communication but also required during control plane signaling. BF is even a more critical requirement during the initial cell discovery phase, when the received signal power is often well below the noise floor.

In addition to BF, Low latency is also one of the fundamental requirements for 5G [4]. Low latency can be achieved by incorporating a high bandwidth sub-carrier. However, this increase in the bandwidth requires higher sampling frequency for an analog-to-digital converter (ADC) which corresponds to a higher power consumption. This power consumption and latency product is even more critical during initial cell discovery (due to large search delays) and directly dictates the choice of an appropriate BF scheme (especially at the MS's receiver design).

Analog, Digital and Hybrid beamforming (ABF, DBF and HBF) are the commonly discussed BF schemes for mmW communication [5]. The choice of an appropriate BF scheme is critically related to its power consumption, and it is even of more importance for a mmW receiver design especially at the mobile station (MS) which has limited available battery. In general, DBF requires a separate RF chain for each antenna element and therefore has the highest power consumption, whereas ABF consumes the least power. However, DBF allows to form multiple simultaneous beams to cover the whole angular space at a particular instant, whereas ABF only converges to a single beam at a particular time instant. Therefore, ABF results in a larger time delay than DBF or HBF due to an additional time required to form beams in different directions to cover the whole angular space. This shows a trade-off among the power consumption and the directional search delay, which is critical during initial cell discovery (ICD). In this work, we study this trade-off and identify the appropriate BF scheme at the MS for ICD.

A. Related Work

The research related to directional cell discovery in mmW 5G cellular networks is very recent. The authors in [6] suggested to scan the complete angular space sequentially to identify the best BF direction both at the MS and the base station (BS). In [7], directional cell discovery is studied, and the authors showed that DBF with a low-bit ADC at the MS can be preferable compared to the ABF. A delay based comparison for initial access in mmW cellular networks is studied in [8], where it is shown that DBF has a lower delay than ABF without any performance degradation. In [9], the advantages of HBF in terms of lower delay and better access probability than ABF are presented for the case of initial beamforming.

To address the issue of large search delay regarding the identification of the right BF direction, a context information (CI) based directional cell search is proposed in [10]. The authors consider a HetNet scenario where the CI about the MS positioning is forwarded to the mmW BS and then the BS transmits the initial synchronization signals in the provided direction. In [11], to reduce the directional search delay associated with the ABF, the authors consider the availability of

the CI regarding the mmW BS positioning at the MS. They further proposed a phase shifters network (PSN) architecture (which results in a lower power consumption than HBF) to mitigate the effect of erroneous CI.

In [12], the total power consumption based comparison of an ABF and a DBF for the mmW receiver at the MS is studied. Results showed that with low power ADC and a fixed total power consumption budget, DBF may result in a higher capacity than ABF when the channel state information is available at the transmitter. The authors in [13] compare the total power consumption of the ABF, DBF and HBF based receiver architectures considering both a low power and a high power ADC model, and discuss the feasibility of different beamforming schemes for both the MS and the BS and for both data plane and control plane signaling. However, to the best of our knowledge there is no previous work which discusses the choice of an appropriate BF scheme (at the MS's receiver) for ICD considering both the power consumption and the time delay (latency) together for both the non-CI and the CI based scenarios.

In this work, focusing on initial cell discovery (ICD) for the CI and the non-CI based scenario, we study this power consumption vs time delay trade-off and identify the choice of an appropriate BF scheme based on the total energy consumption.

B. Our Work

In this work, we compare the receiver energy consumption associated with different BF schemes during initial cell discovery. Primarily, we focus on an energy consumption comparison among the ABF, DBF, HBF and PSN receiver architectures at the MS. Energy consumption is computed as the product of power and time delay. Power consumption for different beamforming schemes is computed considering similar mmW receiver architectures as in [13], while delay is calculated following a synchronization signaling structure as used in LTE. For power consumption, we consider both a low power ADC (LPADC) and a high power ADC (HPADC) model. We also consider both context information (CI) and non CI based scenarios for initial cell discovery. In CI based initial cell discovery, we consider that the GPS coordinates of the mmW base stations (BS) position are provided to the MS by the microwave BS. We divide the CI based scenario into 1) where the GPS coordinates of the MSs positioning are already available, and 2) where the MS has to acquire its GPS coordinates by using assisted GPS (AGPS) which introduces an additional delay. Moreover, we only consider CI based scenario for AFB, HBF and PSN, as DBF already allows to form multiple beams simultaneously to cover the complete angular space, and therefore CI for DBF will not result in any notable advantage. In the rest of the paper, we refer to non CI based scenario as nCI, CI with GPS coordinates already available, i.e., CI with no delay as CInD, and CI with the delay of acquiring the GPS coordinates as CID. Considering the above mentioned scenarios, we show that

- All BF schemes have a similar time delay for CInD scenario, whereas in other scenarios DBF has a minimum delay.
- Energy consumption (EC) of all beamforming schemes decreases with an increase in the sub-carrier bandwidth.
- ABF (for both LPADC and HPADC) only results in a lower EC with a CI based scheme where the GPS coordinates regarding MSs positioning are already available.
- In all scenarios except CInD, DBF results in a lower EC than ABF and HBF.
- PSN has a lower EC than other BF schemes for higher sub-carrier bandwidth.
- The EC trends among different BF schemes are independent of the number of ADC bits.

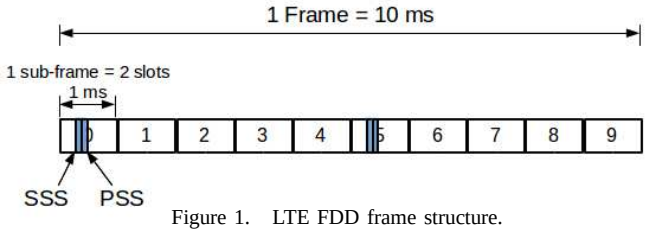

Figure 1. LTE FDD frame structure.

Finally, we propose a new signaling structure for 5G, where the primary synchronization signals are generated with a higher sub-carrier bandwidth while all other signaling is performed at a lower bandwidth. This scheme allows to cover the angular space by the BS with a relatively short delay than with lower sub-carrier bandwidth, and therefore also reduces the energy consumption.

II. Initial Cell Discovery

Initial cell discovery (ICD) procedures proposed for conventional cellular networks are relatively different from what is required for mmW cellular communications. Conventionally, the transmission and the reception of the primary synchronization signals (PSS) and secondary synchronization signals (SSS) (essential for ICD and synchronization) at the BS and the MS, respectively, is done omnidirectionally. However, in mmW cellular networks, directional communication is essential even during the ICD process to exploit the BF gain. In addition to beamforming, reduced latency is another important requirement for 5G cellular networks and this can be achieved by increasing the bandwidth of the sub-carrier B_{SC}. Note that this increase in B_{SC} will also increase the total system bandwidth B_{Tot}. Although an increase in B_{Tot} reduces the latency, it also results in a higher consumption at the mmW receiver, mainly because the ADC needs to sample the incoming signal at a higher rate. We study this power consumption and time delay relationship for different BF schemes. We next discuss the LTE control signaling model to evaluate the synchronization signaling time delay.

A. Initial Cell Discovery in LTE

To initialize the ICD procedure, the MS starts looking for the reception of the synchronization signals (i.e, PSS and SSS).

Table I
SYNCHRONIZATION SIGNAL TIME PERIOD AND TOTAL SYSTEM BANDWIDTH (B_{Tot}) ASSOCIATED TO DIFFERENT B_{SC}

B_{SC} (MHz)	0.015 (LTE)	0.25	0.5	1	10
T_{PSS}	5 ms	0.3 ms	0.15 ms	75 μs	7.5 μs
B_{Tot} (MHz)	1.4	23.3	46.7	93.3	933.3

These synchronization signals provide the initial synchronization and also identify the physical layer cell identity. There are 504 different physical layer cell identities, where the SSS has 168 sequences and provides the cell identity group and the PSS has 3 different sequences and provides identity within the cell identity group. In FDD, the PSS and the SSS are transmitted once every 5 ms for a duration of 71.4 μs (Figure 1). Both synchronization signals constitute 6 resource blocks (corresponds to 72 sub-carriers) with 62 sub-carriers centered around DC (irrespective of the operating bandwidth of LTE) while the rest 10 sub-carriers are unused. After the successful reception of the PSS and the SSS, the MS finishes the initial cell discovery and starts the initial access process.

B. Extension to mmW

Unlike in LTE, in mmW 5G cellular networks an additional requirement for initial cell discovery is to identify the required beamforming direction to improve the SNR at the receiver. In comparison to LTE, this identification of the beamforming direction results in an additional ICD delay. This delay depends on the size of the antenna array and on the beamforming scheme incorporated both at the MS and at the BS. In this work, we consider 64 antennas at the BS and 16 antennas at the MS, which with beamspace beamforming requires $64 \times 16 = 1024$ different directional scans (N_D) to cover the complete angular space. The total ICD delay is a combination of the delay associated with 1) the control signaling (PSS and SSS) and 2) the identification of the beamforming direction.

III. ENERGY CONSUMPTION IN MMW ICD

We measure the energy consumption for different BF schemes considering the three different scenarios discussed in Section I-B. As Energy consumption (EC) is computed as the product of power consumption and time delay, we first compute the time delay associated with nCI, CInD and CID, whereas the power consumption of the different BF schemes will be studied in the following subsections.

A. Time Delay

We follow the LTE signaling structure to calculate the delay associated with the reception of synchronization signals, and identify the delay corresponding to different values of the sub-carrier bandwidth B_{SC}. This delay corresponds to the time period associated to the transmission of the PSS signal, T_{PSS}, for different ICD scenarios, as shown in Table I. To receive the initial synchronization signals, the MS has to look in each BF direction for a duration of T_{PSS}. Therefore, the total time delay t_{Del} can be computed as the product of T_{PSS} and N_D. The total time delay corresponding to different BF schemes and different ICD scenarios is shown in Table II. We consider only ABF at the BS while the MS can form its combining beam using either ABF, DBF, HBF or PSN. This shows that the BS at a particular instant can transmit the synchronization signal only in one angular direction, therefore the BS requires 64 (equal to the number of antennas) different transmissions at separate time instants to cover the whole angular space. Moreover, the angular search delay at the MS is related to the available beamforming scheme.

Table II
t_{Del} FOR DIFFERENT BF SCHEMES CORRESPONDING TO DIFFERENT ICD SCENARIOS, WITH ABF AT THE BS

	t_{Del} (nCI)	t_{Del} (CInD)	t_{Del} (CID)
ABF	$1024 \times T_{PSS}$	$64 \times T_{PSS}$	$64 \times T_{PSS} + t_{CI}$
DBF	$64 \times T_{PSS}$	$64 \times T_{PSS}$	$64 \times T_{PSS}$
HBF	$256 \times T_{PSS}$	$64 \times T_{PSS}$	$64 \times T_{PSS} + t_{CI}$
PSN	$256 \times T_{PSS}$	$64 \times T_{PSS}$	$64 \times T_{PSS} + t_{CI}$

With ABF, the MS has to look in 16 different angular directions, which results in $N_D = 64 \times 16 = 1024$, the maximum scan search delay. Unlike ABF, N_D for HBF (PSN) is directly related to the number of available RF chains (combiners). In this work, the number of RF chains and combiners for HBF and PSN is set to 4. This allows both architectures to form 4 simultaneous beams in different angular directions, and therefore $N_D = 64 \times 16/4 = 256$ for both HBF and PSN. Finally, DBF only requires 64 directional scans to cover the complete angular space. The above mentioned N_D corresponds to the nCI scenario, and t_{Del} can be computed as the product of N_D and T_{PSS} (Table II). This t_{Del} nCI showed that DBF has the least delay whereas ABF results in maximum delay.

We consider the availability of CI only for ABF, HBF and PSN, as the fully digital architecture in DBF allows to form beams in all angular directions simultaneously, and therefore CI will not provide any significant advantage with DBF receivers. The availability of CI is advantageous for ABF, HBF and PSN as it reduces the number of directional scans. With the availability of CI with no delay (i.e., CInD), the receiver already has the knowledge of the appropriate combining direction and therefore the number of directional scans for ABF, HBF and PSN with CInD is similar to that for DBF (i.e., 64). This shows that t_{Del} for CInD for all beamforming schemes is similar.

Finally, a scenario where the GPS coordinates of the MS are not available (i.e., CID) results in an additional time delay. To acquire the GPS coordinates, we considered an AGPS protocol in which the time delay t_{CI} corresponding to the acquisition GPS coordinates is generally communication channel dependent. However, to simplify the analysis we consider the Time to first fix (TTFF) with AGPS to be approximately around 1 s (as mentioned in [14]), and assume $t_{CI} = 1.5$ s, slightly more than TTFF. This is a relatively short delay, however, we show that even this short t_{CI} results not only in a higher delay but also in a relatively higher energy consumption compared to the other design choices.

Table III
RECEIVER POWER CONSUMPTION FOR DIFFERENT BF SCHEMES FOR HPADC

B_{SC}	DBF	ABF	HBF	PSN
15 KHz	1.31	1	2.43	2.49
250 KHz	1.87	1.03	2.57	2.52
500 KHz	2.57	1.07	2.72	2.56
1 MHz	3.67	1.15	3.02	2.63
10 MHz	25.1616	2.4891	8.369	3.978

Table IV
RECEIVER POWER CONSUMPTION FOR DIFFERENT BF SCHEMES FOR LPADC

B_{SC}	DBF	ABF	HBF	PSN
15 KHz	1.28	0.996	2.43	2.3
250 KHz	1.3	0.998	2.43	2.3
500 KHz	1.32	0.999	2.44	2.3
1 MHz	1.37	1	2.45	2.31
10 MHz	2.22	1.06	2.66	2.36

B. Power Consumption

Receiver power consumption is an important concern due to the utilization of huge bandwidths at mmW communication. In this work, we consider the total power consumption of the receiver. The power consumption of all other components except ADC is considered independent of the total system bandwidth. We consider two different power consumption models for an ADC, i.e., a low power and a high power ADC, to better quantify the energy consumption of different beamforming schemes at these two power extremes. For details regarding the receiver architecture and power consumption for different beamforming schemes the reader is referred to [11], [13].

The total system bandwidth (as shown in Table I) is an important parameter, as an increase in B_{Tot} linearly increases the ADC power consumption (as B_{Tot} defines the required sampling rate of an ADC). B_{Tot} is directly proportional to the sub-carrier bandwidth. An increase in B_{SC} results in a higher B_{Tot} and therefore a higher ADC power consumption. B_{Tot} for different B_{SC} is computed following the LTE format used for the 1.4 MHz bandwidth. With 1.4 MHz of bandwidth, 6 RBs are transmitted at each time instant. A RB consists of 12 sub-carriers with B_{SC} = 15 KHz. This corresponds to a bandwidth of 1.08 MHz for 6 RBs, and therefore with total bandwidth of 1.4 MHz, the utilized bandwidth is 77.14% (i.e., $1.08 \text{ MHz} \times 100/1.4 \text{ MHz} = 77.14\%$). B_{Tot} for different B_{SC} can be computed similarly and is listed in Table I.

The power consumption (in Watts) of different beamforming corresponding to different B_{SC} for a HPADC and a LPADC is listed in Table III and Table IV, respectively. The power consumption values are obtained for a 6 bits ADC. The listed values show that the rate of increase in the power consumption is related not only to an increase in B_{Tot} but also to the choice of the ADC design. For instance, the rate at which power consumption increases for HPADC is much higher as compared to LPADC. Moreover, DBF with LPADC results in a lower power consumption than HBF and PSN even for $B_{Tot} = 10$ MHz.

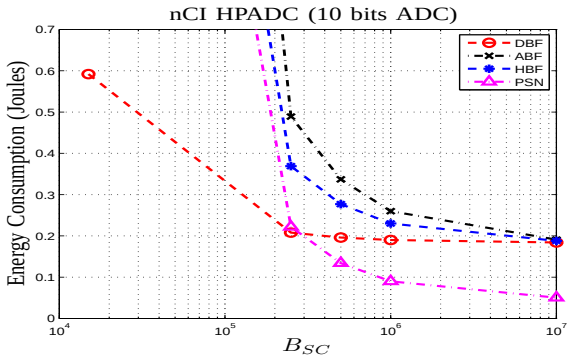

Figure 2. Energy consumption vs B_{SC} for different beamforming schemes with nCI scenario and HPADC.

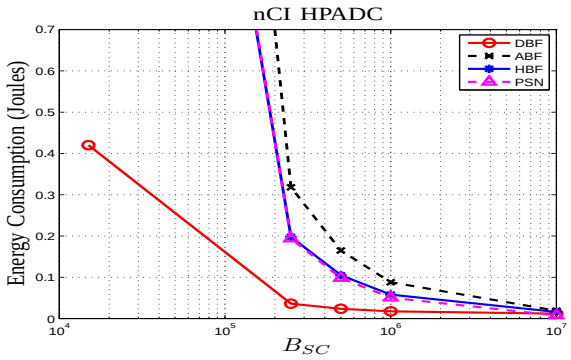

Figure 3. Energy consumption vs B_{SC} for different beamforming schemes with nCI scenario and HPADC.

Finally, the energy consumption (EC) can be computed by evaluating the product of the total power consumption and the time delay.

IV. RESULTS

We now discuss the energy consumption trend followed by different BF receiver architectures during the ICD, and identify the choice of the appropriate BF scheme for nCI, CInD and CID scenarios while considering both a low power and a high power ADC model. The energy consumption of different BF schemes considering different B_{SC} is computed using the power consumption and time delay values listed in Tables III, IV and II, respectively. All results except those in Figure 2 (where we considered 10 bits) are obtained for a 6 bits ADC.

Figures 2, 3 and 4 show the energy consumption vs B_{SC} for the nCI scenario. The plots show that the energy consumption of all BF schemes decreases (with a decreasing slope) with an increase in B_{SC}[1]. This follows from the fact that t_{Del} decreases with an increase in B_{SC}, therefore the EC of the receiver components other than ADC decreases. However, the EC of an ADC remains constant as the power consumption of the ADC increases with the same rate with which t_{Del} decreases. The plots also show that, even with a single RF chain, ABF results in a higher EC relative to the other beamforming

[1] the plots of Figures 5-8 also show a similar trend i.e., decrease in the EC with an increase in the B_{SC}

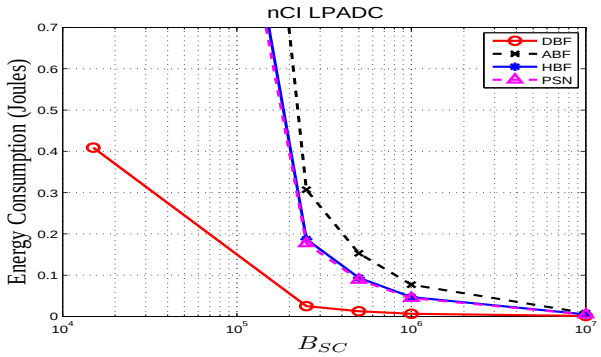

Figure 4. Energy consumption vs B_{SC} for different beamforming schemes with nCI scenario and LPADC.

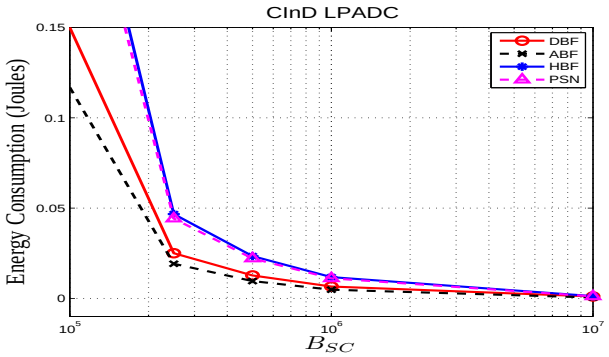

Figure 6. Energy consumption vs B_{SC} for different beam with CInD scenario and LPADC.

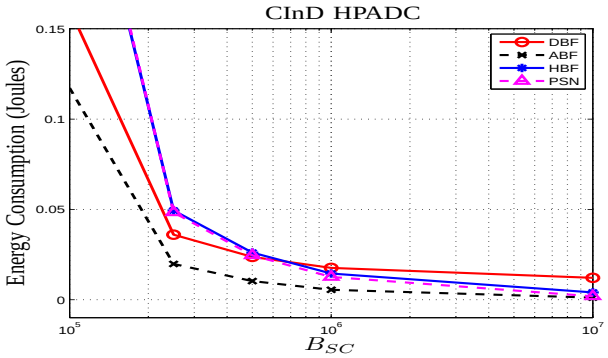

Figure 5. Energy consumption vs B_{SC} for different beamforming schemes with CInD scenario and HPADC.

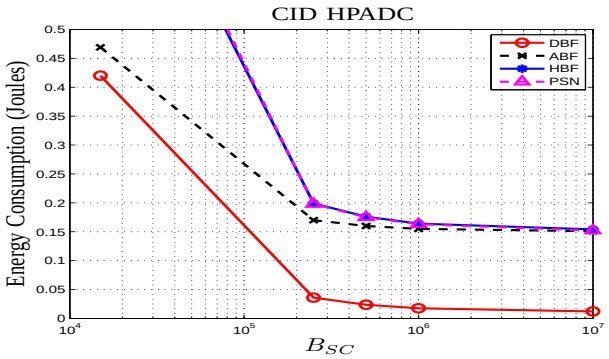

Figure 7. Energy consumption vs B_{SC} for different beam with CID scenario and HPADC.

for both the HPADC and the LPADC model. This shows that t_{Del} for ABF is large enough (due to higher N_D) to dominate the lower power consumption of the ABF which results in the highest EC for ABF. On the other hand, interestingly, DBF always has a lower EC than ABF and HBF, irrespective of the number of ADC bits and of the ADC power model. However, the difference among the EC of DBF, ABF and HBF decreases with an increase in B_{SC} and starts converging to a similar EC. We will discuss this convergence later.

The EC trend followed by PSN is relatively different than what is observed for other BF schemes. Firstly, PSN has a higher energy consumption than DBF at lower B_{SC}, but results in a lower EC than DBF at higher B_{SC}. The converging value of the EC of PSN is also low compared to other BF schemes. This is because the PSN architecture requires ADCs similar to ABF but with much fewer N_D. Secondly, the intersection point between DBF and PSN shifts towards lower B_{SC} with an increase in the number of ADC bits. This is because an increase in bits results in a higher ADC power, due to which the ADC power starts dominating the power consumption of the other components, which results in a rapid convergence in the EC of PSN. Finally, from Figures 2 and 3 it is obvious that the trend among different BF schemes is valid irrespective of the number of ADC bits.

Figures 5 and 6 show an EC comparison among different BF schemes for a CInD scenario. In this scenario, it is considered that the GPS coordinates of the MS are already available and therefore all BF schemes have a similar t_{Del}. The plots show that ABF has the lowest EC in this scenario. This is due to the reduction in N_D thanks to the availability of CI regarding the direction of the mmW BS. Also note that, despite the availability of CI, DBF has a lower or similar EC compared to PSN and HBF up to $B_{SC} = 10$ MHz and $B_{SC} = 1$ MHz for a LPADC model and a HPADC, respectively. The trend among HBF and PSN is similar to what was observed for the nCI scenario. Although these results depict the feasibility of ABF for ICD considering the CInD scenario, to better analyze the feasibility of ABF it is also important to note that the performance of ABF degrades with an increase in the error in the available CI, where PSN has a more robust performance (as shown in [11]). Therefore the choice of the appropriate BF scheme for the CInD scenario not only depends on the minimum EC but is also important to quantify the performance of a particular BF scheme in the case of erroneous CI.

Figures 7 and 8 show the EC vs B_{SC} for a CID scenario. To compute the additional EC corresponding to the acquisition of the GPS coordinates of the MS, the time delay is considered to be 1.5 s (as mentioned in Section III-A) and the power consumption is assumed to be 100 mW. The results show that ABF has a lower EC than HBF and PSN for small values of B_{SC}, but the EC of ABF, HBF and PSN is higher compared to what observed for nCI and CInD scenarios. This is because the EC associated to the acquisition of GPS coordinates is high enough that all BF schemes result in a higher EC. Moreover,

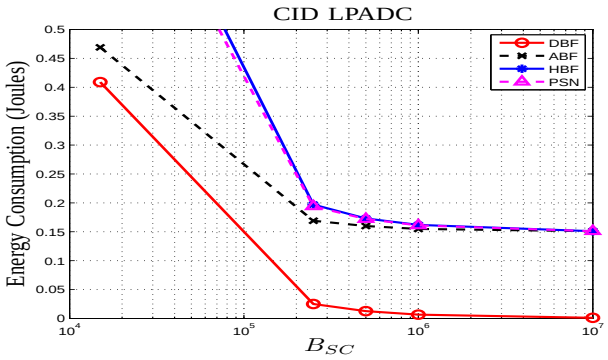

Figure 8. Energy consumption vs B_{SC} for different beam with CID scenario and LPADC.

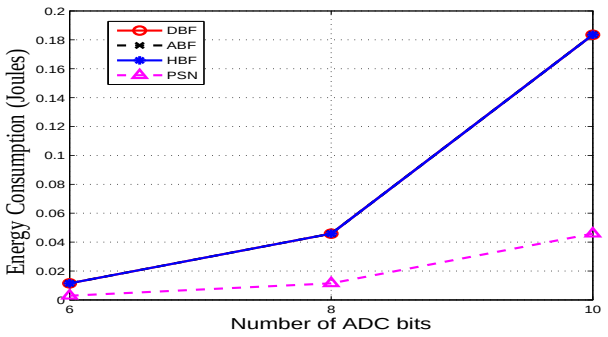

Figure 9. Energy consumption convergence for different BF schemes.

DBF (for both HPADC and LPADC model) has a lower EC than other schemes for all values of B_{SC}. Therefore, the CID scenario not only results in a higher EC for ABF, HBF and PSN but also introduces an extra time delay.

A. EC Convergence

A common trend that can be observed in Figures 2-8 is the convergence of the EC with an increase in B_{SC}. This is because the time delay is higher at lower B_{SC}, which makes the EC of all components other than the ADC more significant. However, with an increase in B_{SC} the EC of the ADC starts dominating. Therefore, the convergence value for the nCI scenario (convergence for CID and CInD can be computed similarly) can simply be calculated by evaluating the EC of the total number of ADCs present in a particular BF scheme. The EC of a single ADC can be computed as

$$E_{ADC} = P_{ADC} \times t_{Del} = cBR \times t_{Del} \quad (1)$$

where E_{ADC} and P_{ADC} are the energy and power consumption of an ADC, c is the energy consumption per conversion and R is the resolution of an ADC. Equation (1) shows that the EC of an ADC remains constant irrespective of B_{SC}, as an increase in B_{SC} will decrease t_{Del} and vice-versa. The convergence value of a particular BF scheme can be found by computing the product E_{ADC} and the number of ADC based on a particular BF scheme. The results for EC convergence are shown in Figure 9, where the convergence value is shown for different numbers of ADC bits while considering ABF, DBF, HBF and PSN schemes. The results show that PSN has the minimum value of the EC convergence for any number of ADC bits, whereas all other beamforming schemes converge to the same value. This is because the product of N_D and the number of ADC for ABF, DBF and HBF has a similar result. However, a PSN architecture which allows to form multiple simultaneous beams and compare them in the analog domain requires a single RF chain (i.e., similar number of ADCs as used for ABF) and can cover the complete angular space with fewer directional scans than ABF, and therefore PSN results in a lower EC.

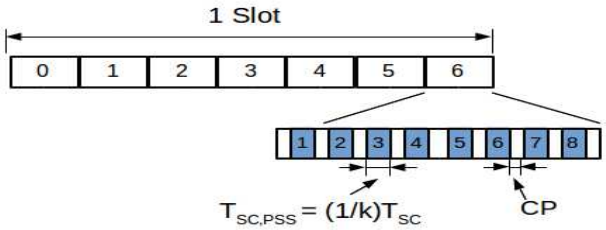

Figure 10. Proposed slot structure for PSS.

V. Higher Sub-Carrier B for PSS Signaling

Usually, control plane signaling requires a lower bandwidth compared to data plane signaling. For instance, in LTE the reserved bandwidth for synchronization signaling is limited to 1.4 MHz, whereas the total system bandwidth can be as large as 20 MHz based on the data rate requirement of the mobile user. The lower bandwidth definitely reduces the power consumption. However, as already shown, an increase in the sub-carrier frequency not only reduces the initial cell search delay but also the EC. By combining the above two points i.e., 1) the difference in the bandwidth of data plane and control plane signaling and 2) a higher sub-carrier bandwidth results in a lower latency and EC, we now propose a new signaling structure for 5G cellular networks, where PSS utilizes a relatively higher sub-carrier bandwidth compared to other signaling. The maximum increase in the PSS sub-carrier bandwidth ($B_{SC,PSS}$) can be set to the maximum available bandwidth for data plane. We next discuss the proposed signaling structure and briefly discuss its performance, whereas a detailed analysis is left as future work.

The proposed slot structure for 5G containing PSS is shown in Figure 10, where $T_{SC,PSS}$ and T_{SC} represents the time period of the higher bandwidth PSS sub-carrier and sub-carrier bandwidth (i.e., B_{SC}) used for other signaling, respectively, CP represents the cyclic prefix interval corresponding to $T_{SC,PSS}$ and k is a constant which represents the fractional increase or decrease in B_{SC} or T_{SC} for the PSS. In Figure 10, k is set to 8, and therefore in the time duration T_{SC}, 8 primary synchronization signals can be transmitted. This is because, according to the proposed structure, $B_{SC,PSS}$ is increased k times, which reduces the transmission time required for PSS by a factor of k compared to what is required for sub-carriers with bandwidth B_{SC}. The allows to transmit multiple $B_{SC,PSS}$

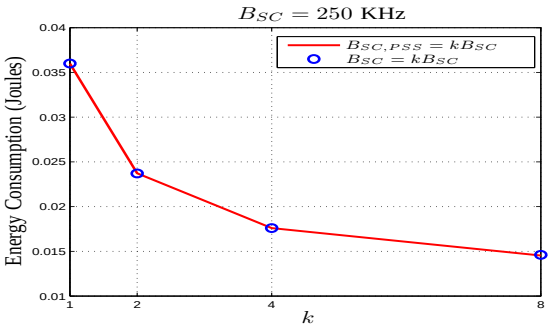

Figure 11. Proposed slot structure for PSS.

signals in either a different or the same angular direction in a similar time interval as that of other signaling, i.e., T_{SC}. This has two main advantages, 1) k PSS signals can be transmitted in the same angular direction to capture higher energy in a reduced time, and 2) to transmit k PSS signal into different angular direction to reduce the search delay (in this work we only discuss the latter.).

According to the proposed scheme, the reduction in the directional search delay with higher $B_{SC,PSS}$ compared to B_{SC} can be given as

$$t_{Del,Red} = \frac{t_{Del}}{k} \tag{2}$$

where $t_{Del,Red}$ is a reduced delay. Note that this reduced delay is similar as we get with for k times higher (fixed) sub-carrier bandwidth for all signaling. However, with the proposed structure (assuming ABF), the BS can transmit k PSS signals in consecutive time instant in k different direction whereas with same B_{SC} the BS can transmit PSS only in a single direction every T_{PSS}. We next discuss the EC vs k relationship.

Figure 11 shows the EC for different values of k. The plot shows that the EC reduces with an increase in k, and therefore the propose signaling structure indeed reduces the EC. Moreover, the reduction in EC is similar to what can be achieved by using a fixed higher bandwidth sub-carrier for all signaling, as total time delay for both cases is similar. Therefore, the proposed structure with higher $B_{SC,PSS}$ can achieve a low EC (similar to what can be achieved with a higher B_{SC}), without increasing B_{SC} for other signaling (which allows ADC to operate at lower sampling rate especially during data communication which reduces the power consumption).

VI. Conclusions

We studied the directional initial cell discovery problem for mmW 5G cellular networks in the context of an energy consumption comparison of ABF, DBF, HBF and PSN schemes. We considered both context information (CInD, CID) and non context information (nCI) based scenario. We showed that the perception regarding the higher energy consumption of DBF is not true during the directional initial cell discovery phase. Rather, DBF has a lower energy consumption than ABF and HBF with much lower angular search delay for both CID (i.e., context information with delay) and nCI scenarios. Moreover, the recently proposed PSN architecture has a lower energy consumption than other beamforming schemes at higher sub-carrier bandwidth for nCI scenario, whereas ABF has minimum energy consumption in the CInD (i.e., CI with no delay) scenario. We also showed that energy consumption results presented in this work (especially related to ABF, DBF and HBF) are valid irrespective to the number of ADC bits. Finally, we proposed a new signaling structure which utilize a relatively higher bandwidth sub-carrier for PSS compared to other signaling which reduces the latency and energy consumption during initial cell discovery.

In the future, we will study the bandwidth vs noise power trade-off and identify the regimes where the energy consumption and the detection probability is maximized.

References

[1] Z. Pi and F. Khan, "An introduction to millimeter-wave mobile broadband systems," *IEEE Communications Magazine*, vol. 49, no. 6, pp. 101–107, Jun. 2011.

[2] T. Rappaport, S. Sun, R. Mayzus, H. Zhao, Y. Azar, K. Wang, G. Wong, J. Schulz, M. Samimi, and F. Gutierrez, "Millimeter wave mobile communications for 5G cellular: It will work!" *IEEE Access*, vol. 1, pp. 335–349, 2013.

[3] W. Roh, J.-Y. Seol, J. Park, B. Lee, J. Lee, Y. Kim, J. Cho, K. Cheun, and F. Aryanfar, "Millimeter-wave beamforming as an enabling technology for 5G cellular communications: theoretical feasibility and prototype results," *IEEE Communications Magazine*, vol. 52, no. 2, pp. 106–113, February 2014.

[4] J. G. Andrews, S. Buzzi, W. Choi, S. V. Hanly, A. Lozano, A. C. K. Soong, and J. C. Zhang, "What will 5G be?" *IEEE Journal on Selected Areas in Communications*, vol. 32, no. 6, pp. 1065–1082, Jun. 2014.

[5] S. Sun, T. S. Rappaport, R. W. Heath, A. Nix, and S. Rangan, "MIMO for millimeter-wave wireless communications: beamforming, spatial multiplexing, or both?" *IEEE Communications Magazine*, vol. 52, no. 12, pp. 110–121, Dec. 2014.

[6] C. Jeong, J. Park, and H. Yu, "Random access in millimeter-wave beamforming cellular networks: issues and approaches," *IEEE Communications Magazine*, vol. 53, no. 1, pp. 180–185, Jan. 2015.

[7] C. Barati, S. Hosseini, S. Rangan, P. Liu, T. Korakis, S. Panwar, and T. Rappaport, "Directional cell discovery in millimeter wave cellular networks," *IEEE Transactions on Wireless Communications*, vol. 14, no. 12, pp. 6664–6678, Dec. 2015.

[8] C. N. Barati, S. A. Hosseini, M. Mezzavilla, S. Rangan, T. Korakis, S. S. Panwar, and M. Zorzi, "Directional initial access for millimeter wave cellular systems," *CoRR*, vol. abs/1511.06483, 2015. [Online]. Available: http://arxiv.org/abs/1511.06483

[9] V. Desai, L. Krzymien, P. Sartori, W. Xiao, A. Soong, and A. Alkhateeb, "Initial beamforming for mmwave communications," in *48th Asilomar Conference on Signals, Systems and Computers*, Nov 2014, pp. 1926–1930.

[10] A. Capone, I. Filippini, and V. Sciancalepore, "Context information for fast cell discovery in mm-wave 5G networks," in *Proceedings of 21th European Wireless Conference*, May 2015.

[11] W. b. Abbas and M. Zorzi, "Context information based initial cell search for millimeter wave 5G cellular networks," in *Proceedings of 25th European Conference on Networks and Communications, EuCNC, 2016*, To appear. [Online]. Available: http://arxiv.org

[12] O. Orhan, E. Erkip, and S. Rangan, "Low power analog-to-digital conversion in millimeter wave systems: Impact of resolution and bandwidth on performance," in *Information Theory and Applications Workshop (ITA)*, Feb. 2015, pp. 191–198.

[13] W. b. Abbas and M. Zorzi, "Towards an appropriate receiver beamforming scheme for millimeter wave communication: A power consumption based comparison," in *Proceedings of 22nd European Wireless Conference, 2016*, To appear. [Online]. Available: http://arxiv.org

[14] F. V. Diggelen, *A-GPS: Assisted GPS, GNSS, and SBAS*, 2009.